A chi-square type test for time-invariant fiber pathways of the brain: HARDI extension

Juna Goo[1] and Lyudmila Sakhanenko[2]

[1]Department of Mathematics, Boise State University
[2]Department of Statistics and Probability, Michigan State University

Abstract
Integral curve estimation is a well-established method for reconstructing in vivo nerve fiber pathways in the white matter of the brain. Using longitudinal high angular resolution diffusion imaging (HARDI) data, we formulate the longitudinal ensemble of fiber trajectories as an integral curve with the parameter time. The goal of this article is to develop a test statistic to determine whether there are anatomically plausible changes in nerve fibers with two directions, such as crossing, kissing, or bending fibers. We envision that rejecting the null hypothesis could help identify a potential anatomical biomarker for neurodegenerative diseases, such as Alzheimer's disease.

Key Words: Diffusion-weighted magnetic resonance imaging, Integral curve, Kernel smoothing

1. Introduction

Alzheimer's disease (AD) is an age-related neurodegenerative brain disorder, which is the most prevalent cause of dementia [13]. AD can develop from mild cognitive impairment (MCI), a stage in which cognitive decline extends beyond healthy aging. The main difference between MCI and AD is whether cognitive impairment is severe enough to interfere with daily tasks [1]. Although there is no universal laboratory test that can determine the progression of AD in patients with MCI, diffusion-weighted magnetic resonance imaging (dMRI) has been pivotal in the early diagnosis and progression of AD.

There are two popular techniques for modeling fiber tracts in vivo based on dMRI: diffusion tensor imaging (DTI) and high angular resolution diffusion imaging (HARDI). In the early 1990s, DTI was introduced to characterize water movement at a location using a 3×3 symmetric and positive definite matrix, which is termed the "diffusion tensor" [2]. DTI estimates anatomically plausible fiber trajectories in the white matter of the brain, assuming that the leading eigenvector of the diffusion tensor associated with the largest eigenvalue is parallel to the local fiber tract orientation. The estimation of white matter fiber tracts using DTI has been extensively studied [3, 4, 7, 11, 12, 15].

However, DTI averages the diffusion properties of water molecules within a voxel, making it unable to capture different fiber tract orientations. HARDI was introduced to overcome the artifacts of DTI by using more distinct spatial directions than DTI [17]. Unlike DTI, HARDI characterizes water diffusion using a high-order supersymmetric and positive definite tensor [9, 14]. In order to determine different fiber orientations, one can use pseudo-eigenvectors of the high-order tensor that correspond to pseudo-eigenvalues [6, 18].

This article focuses on the longitudinal HARDI framework. Longitudinal models allow researchers to investigate whether neural connectivity deteriorates over time due to disease progression or brain injury [5, 16]. Recently, a chi-square type test was proposed to examine time-dependent anatomical changes in a region of the brain based on the longitudinal DTI model [10]. The null hypothesis in [10] corresponds to a zero rate of change with respect to time in the longitudinal ensemble of fiber trajectories that are uniformly oriented.

This article extends the framework of [10] to the one for longitudinal high angular resolution diffusion imaging (HARDI) studies. Our goal is to develop a statistical test to examine time-dependent changes in local fiber tracts with two directions, such as crossing, kissing, or bending fibers.

2. Framework

Let $D \in \mathbb{R}^{3^M}$ denote a supersymmetric and positive definite high-order tensor of rank R and even order $M > 2$. When $M = 2$, D is the same as the diffusion tensor in DTI. R denotes the maximum number of fiber directions per voxel. Following [18], the best rank-1 approximation of the tensor D is defined as follows:

$$\lambda \underbrace{v \otimes v \otimes \cdots \otimes v}_{M\text{times}} = \lambda v^{\otimes M}$$

where $\otimes$ denotes the tensor product, $\lambda > 0$ is an unknown scalar and $v \in \mathbb{R}^3$ is an unknown unit vector (i.e., $\|v\| = 1$). Here, we wish to find (λ, v) that minimizes the following Frobenius norm:

$$\|D - \lambda v^{\otimes M}\|_F^2. \tag{1}$$

Solving the pair (λ, v) requires an iterative method starting from the initial values (λ_0, v_0). Let $(\lambda^{(1)}, v^{(1)})$ denote the solution to the best rank-1 approximation of the tensor $D^{(1)} = D$. For $r = 2, \ldots, R$, we define $(\lambda^{(r)}, v^{(r)})$ that make up the best rank-1 approximation of the tensor

$$D^{(r)} = D^{(r-1)} - \lambda^{(r-1)}(v^{(r-1)})^{\otimes M}. \tag{2}$$

See [18] and references therein for details. $\lambda^{(r)}$ is termed the rth pseudo-eigenvalue and $v^{(r)}$ is termed the rth normalized pseudo-eigenvector of the tensor D for $r = 1, \ldots, R$.

Then we have the following assumption:

Assumption 1 *Let $\mathcal{G}$ denote a compact set with Lebesgue measure 1 in $\mathbb{R}^3$. $D(u), u \in \mathcal{G}$ is a supersymmetric, twice continuously differentiable, and positive definite high-order tensor of rank R and even order $M > 2$.*

Throughout this article, we assume $R = 2$ (two fiber directions per voxel). Let $T \in \mathbb{R}^+$. For $r = 1, 2$, we define the rth fiber trajectory at time $t \in [0, T]$ as an integral curve $x^{(r)}(s, t)$ which is the solution to the following ordinary differential equation with the parameter time $t \in [0, T]$:

$$\frac{\partial}{\partial s} x^{(r)}(s, t) = v^{(r)}(x^{(r)}(s, t)), \quad x^{(r)}(0, t) = x_0, \tag{3}$$

where $x_0 \in \mathcal{G}$ is a time-invariant initial value, $s \in [0, S], S \in \mathbb{R}^+$ is the arc length along the curve, and $t \in [0, T]$ plays a role of the parameter in its differential equation. $v^{(r)}(x^{(r)}(s, t))$ denotes the rth normalized pseudo-eigenvector of the tensor $D(u)$, where $x^{(r)}(s, t)$ is plugged into u.

The equation (3) is equivalent to

$$x^{(r)}(s, t) = x_0 + \int_0^s v^{(r)}(x^{(r)}(\xi, t))d\xi. \tag{4}$$

The solution $x^{(r)}(s, t)$ is unique and stays in $\mathcal{G}$ [8].

In this article, we aim to develop a test statistic to determine whether there are anatomically plausible changes in local fiber tracts with two directions, such as crossing, kissing, or bending fibers. We note that the cosine of an angle θ between two tangent lines to the curves at the arc

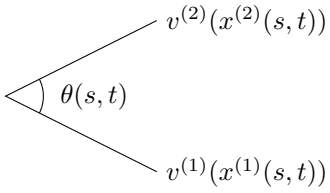

Figure 1: the angle between two tangent lines to the curves at the arc length s and time t

length s and time t can be defined as follows:

$$\cos(\theta(s,t)) = \langle v^{(1)}(x^{(1)}(s,t)), v^{(2)}(x^{(2)}(s,t))\rangle \tag{5}$$

since $v^{(r)}(u), r = 1, 2$ is the rth normalized pseudo-eigenvector of the tensor $D(u)$.

Let $J_M = (M+1)(M+2)/2$. Let $\underline{\mathbf{D}} \in \mathbb{R}^{J_M}$ be the vectorization of the supersymmetric tensor $D \in \mathbb{R}^{3^M}$. For $r = 1, 2$, let

$$\nabla v^{(r)}(x^{(r)}(s,t)) = \left.\frac{\partial v^{(r)}(u)}{\partial \underline{\mathbf{D}}(u)}\right|_{u=x^{(r)}(s,t)}$$

be a $3 \times J_M$ matrix-valued function and

$$\nabla \underline{\mathbf{D}}(x^{(r)}(s,t)) = \left.\frac{\partial \underline{\mathbf{D}}(u)}{\partial u}\right|_{u=x^{(r)}(s,t)}$$

be a $J_M \times 3$ matrix-valued function.

If the cosine of the angle between them does not change over time t, then we have

$$\begin{aligned}\frac{\partial}{\partial t}\cos(\theta(s,t)) = &\langle \nabla v^{(1)}(x^{(1)}(s,t)) \nabla \underline{\mathbf{D}}(x^{(1)}(s,t)) \frac{\partial}{\partial t} x^{(1)}(s,t), v^{(2)}(x^{(2)}(s,t))\rangle \\ &+ \langle v^{(1)}(x^{(1)}(s,t)), \nabla v^{(2)}(x^{(2)}(s,t)) \nabla \underline{\mathbf{D}}(x^{(2)}(s,t)) \frac{\partial}{\partial t} x^{(2)}(s,t)\rangle = 0.\end{aligned}$$

Let $\begin{bmatrix} x^{(1)}(s,t) \\ x^{(2)}(s,t) \end{bmatrix}$ be a 6×1 stacked vector. Then testing whether the angle between two fiber directions remains constant over time can be achieved by testing the following hypothesis:

$$H_0 : \frac{\partial}{\partial t}\begin{bmatrix} x^{(1)}(s,t) \\ x^{(2)}(s,t) \end{bmatrix} = 0_6 \text{ against } H_1 : \frac{\partial}{\partial t}\begin{bmatrix} x^{(1)}(s,t) \\ x^{(2)}(s,t) \end{bmatrix} \neq 0_6$$

since the null hypothesis (H_0) implies $\partial\cos(\theta(s,t))/\partial t = 0$.

3. Estimation

For each $u \in \mathcal{G}$, let $y(u,g)$ denote the observed image signal affected by water diffusion along a spatial direction $g \in \mathbb{R}^3$, $\|g\| = 1$, and $y_0(u)$ denote the observed image signal without any magnetic field gradient. The log-losses of the signal can be observed in the acquired raw dMRI data and can be modeled as follows [9, 14]:

$$\log\left(\frac{y(u,g)}{y_0(u)}\right) = -c \sum_{i_1=1}^{3} \cdots \sum_{i_M=1}^{3} D_{i_1 \ldots i_M}(u) g_{i_1} \ldots g_{i_M} + \sigma(u,g)\xi_g, \tag{6}$$

where the constant c depends only on the gyromagnetic ratio of hydrogen, the gradient pulse sequence shape, duration and other timing parameters of the imaging procedure, each of which are known *a priori*, $\sigma(u,g) > 0$, and ξ_g describes noise. $D_{i_1 \ldots i_M}$ denotes the component of the tensor D.

HARDI requires $N = J_M m$ gradient directions where $J_M = (M+1)(M+2)/2$ and $m \geq 1$. The equation (6) can be rewritten as follows:

$$Y(u) = B\underline{\mathbf{D}}(u) + \Sigma^{1/2}(u)\Xi, \tag{7}$$

where Y is a $N \times 1$ vector obtained by stacking $\log(y(u,g)/y_0(u))$ along N gradient directions, B is a $N \times J_M$ fixed matrix determined from the set of directions, Σ is a $N \times N$ unknown symmetric positive definite matrix, and Ξ is a $N \times 1$ random vector.

In order to accommodate the longitudinal HARDI studies, we let $n = n_x n_t$, where n_x is the number of spatial points in a 3D regular grid and n_t is the number of time points (or the number of visits for the dMRI scan over time). The observations are $(U_i, Y(U_i)), i = 1, \ldots, n$, where U_i's are assumed to be independent and uniformly distributed in $\mathcal{G}$ and

$$Y(U_i) = B\underline{\mathbf{D}}(U_i) + \Sigma^{1/2}(U_i)\Xi_i,$$

where Ξ_i's are independent and identically distributed random vectors in $\mathbb{R}^N$ having a zero mean vector and an identity variance-covariance matrix.

Ordinary or weighted least squares estimators (OLS/WLS) can be used to estimate $\underline{\mathrm{D}}(U_i)$ given U_i. For example, for $i = 1, \ldots, n$, the OLS of $\underline{\mathrm{D}}$ at given U_i is as follows:

$$\begin{aligned}\tilde{\underline{\mathrm{D}}}(U_i) &= (B^\top B)^{-1} B^\top Y(U_i) \\ &= (B^\top B)^{-1} B^\top [B\underline{\mathrm{D}}(U_i) + \Sigma^{1/2}(U_i)\Xi_i] \\ &= \underline{\mathrm{D}}(U_i) + \Gamma_i,\end{aligned}$$

where $\Gamma_i = (B^\top B)^{-1} B^\top \Sigma^{1/2}(U_i)\Xi_i$. Then we define

$$\Sigma_\Gamma(U_i) = \mathbb{E}[\Gamma_i \Gamma_i^\top | U_i] = (B^\top B)^{-1} B^\top \Sigma(U_i) B (B^\top B)^{-1}.$$

Next, a kernel smoothing estimator of $\underline{\mathrm{D}}(u)$ can be defined as follows:

$$\hat{\underline{\mathrm{D}}}_n(u) = \frac{1}{nh_n^3} \sum_{i=1}^{n} K\left(\frac{u - U_i}{h_n}\right) \tilde{\underline{\mathrm{D}}}(U_i), \tag{8}$$

where K is a kernel function and h_n is a bandwidth. We have the following assumption on the kernel function:

Assumption 2 *K is nonnegative and twice continuously differentiable on its bounded support. Moreover, $\int_{\mathbb{R}^3} K(u)du = 1$ and $\int_{\mathbb{R}^3} uK(u)du = 0$.*

Let $\hat{D}_n(u)$ denote a supersymmetric tensor estimator that is reconstructed from $\hat{\underline{\mathrm{D}}}_n(u)$. Let $\hat{\lambda}_n^{(r)}(u)$ and $\hat{v}_n^{(r)}(u)$ denote a pair of the rth pseudo-eigenvalue and (normalized) pseudo-eigenvector estimators that make up the best rank-1 approximation of the tensor estimator. Ultimately, an estimator of the rth fiber trajectory ($r = 1, 2$) at time $t \in [0, T]$ can be defined as follows:

$$\frac{\partial}{\partial s}\hat{x}_n^{(r)}(s,t) = \hat{v}_n^{(r)}(\hat{x}_n^{(r)}(s,t)), \quad \hat{x}_n^{(r)}(0,t) = x_0, \tag{9}$$

which is equivalent to

$$\hat{x}_n^{(r)}(s,t) = x_0 + \int_0^s \hat{v}_n^{(r)}(\hat{x}_n^{(r)}(\xi,t))d\xi. \tag{10}$$

Then $\begin{bmatrix}\hat{x}_n^{(1)}(s,t) \\ \hat{x}_n^{(2)}(s,t)\end{bmatrix}$ denotes an estimator of $\begin{bmatrix}x^{(1)}(s,t) \\ x^{(2)}(s,t)\end{bmatrix}$.

We can also estimate $\Sigma(u)$ in the equation (7) as follows:

$$\hat{\Sigma}_n(u) = \frac{1}{nh_n^3} \sum_{i=1}^{n} K\left(\frac{u - U_i}{h_n}\right) \tilde{\Sigma}(U_i),$$

where $\tilde{\Sigma}(U_i) = [Y(U_i) - B\hat{D}_n(u)][Y(U_i) - B\hat{D}_n(u)]^\top, i = 1, \ldots, n$.

4. Main results

The proofs of main results require the following assumptions:

Assumption 3 *The bandwidth h_n satisfies the condition $nh_n^6 \to \beta$ as $n \to \infty$, where $\beta > 0$ is a known fixed number.*

The proofs of the following lemmas are similar to the one in [10].

Lemma 1 *Assumptions 1-3 hold. Then we have*

$$\sup_{u \in \mathcal{G}} |\hat{\underline{\mathrm{D}}}_n(u) - \underline{\mathrm{D}}(u)| \xrightarrow{P} 0 \quad \text{as} \quad n \to \infty.$$

Lemma 2 *Assumptions 1-3 hold. Then we have*

$$\sup_{u\in\mathcal{G}}|\hat{\Sigma}_n(u)-\Sigma(u)|\xrightarrow{P}0 \quad \text{as} \quad n\to\infty.$$

Lemma 3 *Assumptions 1-3 hold. Then we have*

$$\sup_{u\in\mathcal{G}}|\nabla\hat{\underline{\mathbf{D}}}_n(u)-\nabla\underline{\mathbf{D}}(u)|\xrightarrow{P}0 \quad \text{as} \quad n\to\infty.$$

Lemma 4 *Assumptions 1-3 hold. Then we have*

$$\sup_{s\in[0,S],t\in[0,T]}|\hat{x}_n^{(r)}(s,t)-x^{(r)}(s,t)|\xrightarrow{P}0 \quad \text{as} \quad n\to\infty.$$

In order to prove main theorems, we introduce the following definitions: For $u\in\mathbb{R}^3$, let

$$\Psi(u)=\int_{\mathbb{R}^3}K(z)K(z+u)dz, \quad \psi(u)=\int_{\mathbb{R}}\Psi(\tau u)d\tau.$$

For $r=1,2$, let G_r be a 3×3 Green's function, defined as the solution of the following partial differential equation:

$$\frac{\partial G_r(s,s^*,t)}{\partial s}=\nabla v^{(r)}(x^{(r)}(s,t))\nabla\underline{\mathbf{D}}(x^{(r)}(s,t))G_r(s,s^*,t), \quad G_r(s^*,s^*,t)=\mathbb{I},$$

where $\mathbb{I}$ denotes a 3×3 identity matrix. For the differentiation of the pseudo-eigenvector with respect to the vectorization of the tensor, see Theorem 2 of [6].

Theorem 1 *Assumptions 1-3 hold. At fixed $t\in[0,T]$, the sequence of stochastic processes*

$$\sqrt{nh_n^2}\left(\begin{bmatrix}\hat{x}_n^{(1)}(s,t)\\ \hat{x}_n^{(2)}(s,t)\end{bmatrix}-\begin{bmatrix}x^{(1)}(s,t)\\ x^{(2)}(s,t)\end{bmatrix}\right)$$

converges weakly in the space of $\mathbb{R}^6$-valued continuous functions on $[0,S]$ to the Gaussian process $\mathcal{GP}(s,t), s\in[0,S], t\in[0,T]$ with mean function

$$\begin{bmatrix}\mu_1(s,t)\\ \mu_2(s,t)\end{bmatrix}=\frac{\sqrt{\beta}}{2}\int_0^s\int_{\mathbb{R}^3}\begin{bmatrix}G_1(s,\xi,t)\nabla v^{(1)}(x^{(1)}(\xi,t))K(z)\langle\nabla^2\underline{\boldsymbol{D}}(x^{(1)}(\xi,t))z,z\rangle\\ G_2(s,\xi,t)\nabla v^{(2)}(x^{(2)}(\xi,t))K(z)\langle\nabla^2\underline{\boldsymbol{D}}(x^{(2)}(\xi,t))z,z\rangle\end{bmatrix}dzd\xi$$

and covariance function for $s,s^*\in[0,S]$

$$\begin{bmatrix}C_{11}(s,s^*,t) & O_3\\ O_3 & C_{22}(s,s^*,t)\end{bmatrix},$$

where

$$\begin{aligned}C_{rr}(s,s^*,t)=&\int_0^{s\wedge s^*}\psi(v^{(r)}(x^{(r)}(\xi,t)))G_r(s,\xi,t)\nabla v^{(r)}(x^{(r)}(\xi,t))\\ &\times[\underline{\boldsymbol{D}}(x^{(r)}(\xi,t))\underline{\boldsymbol{D}}^\top(x^{(r)}(\xi,t))+\Sigma_\Gamma(x^{(r)}(\xi,t))]\\ &\times(\nabla v^{(r)}(x^{(r)}(\xi,t)))^\top G_r^\top(s^*,\xi,t)d\xi, \quad r=1,2,\end{aligned}$$

and O_3 denotes a 3×3 matrix of zeros.

Sketch Proof of Theorem 1: Let $y^{(r)}(s,t)=\hat{x}_n^{(r)}(s,t)-x^{(r)}(s,t), r=1,2$. Then we have

$$\begin{aligned}\begin{bmatrix}y^{(1)}(s,t)\\ y^{(2)}(s,t)\end{bmatrix}&=\int_0^s\begin{bmatrix}\hat{v}_n^{(1)}(\hat{x}_n^{(1)}(\xi,t))-v^{(1)}(x^{(1)}(\xi,t))\\ \hat{v}_n^{(2)}(\hat{x}_n^{(2)}(\xi,t))-v^{(2)}(x^{(2)}(\xi,t))\end{bmatrix}d\xi\\ &=\begin{bmatrix}z^{(1)}(s,t)\\ z^{(2)}(s,t)\end{bmatrix}+\begin{bmatrix}\delta^{(1)}(s,t)\\ \delta^{(2)}(s,t)\end{bmatrix},\end{aligned}$$

where

$$\begin{bmatrix} z^{(1)}(s,t) \\ z^{(2)}(s,t) \end{bmatrix} = \int_0^s \begin{bmatrix} \nabla v^{(1)}(x^{(1)}(\xi,t))(\hat{\underline{\mathbf{D}}}_n - \underline{\mathbf{D}})(x^{(1)}(\xi,t)) \\ \nabla v^{(2)}(x^{(2)}(\xi,t))(\hat{\underline{\mathbf{D}}}_n - \underline{\mathbf{D}})(x^{(2)}(\xi,t)) \end{bmatrix} d\xi$$
$$+ \int_0^s \begin{bmatrix} \nabla v^{(1)}(x^{(1)}(\xi,t))\nabla \underline{\mathbf{D}}(x^{(1)}(\xi,t))z^{(1)}(\xi,t) \\ \nabla v^{(2)}(x^{(2)}(\xi,t))\nabla \underline{\mathbf{D}}(x^{(2)}(\xi,t))z^{(2)}(\xi,t) \end{bmatrix} d\xi,$$

$$\begin{bmatrix} \delta^{(1)}(s,t) \\ \delta^{(2)}(s,t) \end{bmatrix} = \int_0^s \begin{bmatrix} \nabla v^{(1)}(x^{(1)}(\xi,t))\nabla \underline{\mathbf{D}}(x^{(1)}(\xi,t))\delta^{(1)}(\xi,t) \\ \nabla v^{(2)}(x^{(2)}(\xi,t))\nabla \underline{\mathbf{D}}(x^{(2)}(\xi,t))\delta^{(2)}(\xi,t) \end{bmatrix} d\xi + R_{12}(s,t),$$

and

$$\begin{aligned} &R_{12}(s,t) \\ &= \int_0^s \begin{bmatrix} \hat{v}_n^{(1)}(\hat{x}_n^{(1)}(\xi,t)) - v^{(1)}(\hat{x}_n^{(1)}(\xi,t)) - \nabla v^{(1)}(x^{(1)}(\xi,t))\nabla \underline{\mathbf{D}}(x^{(1)}(\xi,t))y^{(1)}(\xi,t) \\ \hat{v}_n^{(2)}(\hat{x}_n^{(2)}(\xi,t)) - v^{(2)}(\hat{x}_n^{(2)}(\xi,t)) - \nabla v^{(2)}(x^{(2)}(\xi,t))\nabla \underline{\mathbf{D}}(x^{(2)}(\xi,t))y^{(2)}(\xi,t) \end{bmatrix} d\xi \\ &+ \int_0^s \begin{bmatrix} v^{(1)}(\hat{x}_n^{(1)}(\xi,t)) - v^{(1)}(x^{(1)}(\xi,t)) - \nabla v^{(1)}(x^{(1)}(\xi,t))(\hat{\underline{\mathbf{D}}}_n - \underline{\mathbf{D}})(x^{(1)}(\xi,t)) \\ v^{(2)}(\hat{x}_n^{(2)}(\xi,t)) - v^{(2)}(x^{(2)}(\xi,t)) - \nabla v^{(2)}(x^{(2)}(\xi,t))(\hat{\underline{\mathbf{D}}}_n - \underline{\mathbf{D}})(x^{(2)}(\xi,t)) \end{bmatrix} d\xi. \end{aligned}$$

Using the Green's functions $G_r, r = 1, 2$, we can write

$$\begin{bmatrix} z^{(1)}(s,t) \\ z^{(2)}(s,t) \end{bmatrix} = \int_0^s \begin{bmatrix} G_1(s,\xi,t)\nabla v^{(1)}(x^{(1)}(\xi,t))(\hat{\underline{\mathbf{D}}}_n - \underline{\mathbf{D}})(x^{(1)}(\xi,t)) \\ G_2(s,\xi,t)\nabla v^{(2)}(x^{(2)}(\xi,t))(\hat{\underline{\mathbf{D}}}_n - \underline{\mathbf{D}})(x^{(2)}(\xi,t)) \end{bmatrix} d\xi.$$

As similar to the proof in [10], the following can be proven:

$$\sqrt{nh_n^2} \begin{bmatrix} z^{(1)}(s,t) \\ z^{(2)}(s,t) \end{bmatrix} \Rightarrow \mathcal{GP}(s,t), s \in [0,S], t \in [0,T],$$

via the functional central limit theorem, and it can be proven that:

$$\sup_{s\in[0,S],t\in[0,T]} \left| \begin{bmatrix} \delta^{(1)}(s,t) \\ \delta^{(2)}(s,t) \end{bmatrix} \right| = o_p\left(\frac{1}{\sqrt{nh_n^2}}\right).$$

The mean $\mu_r(s,t)$ and covariance functions $C_{rr}(s,s^*,t)$ for $r = 1, 2$, can be derived as in the proof of [10]. The zero cross-covariance can be proven as follows: Let $\psi = \frac{x^{(1)}(\xi,t)-U}{h_n}$. Then we have

$$\begin{aligned} &Cov[z^{(1)}(s,t), z^{(2)}(s^*,t)] \\ &= \frac{1}{nh_n^3} \int_0^s \int_0^{s^*} \int_{\mathbb{R}^3} G_1(s,\xi,t)\nabla v^{(1)}(x^{(1)}(\xi,t))K(\psi)K\left(\psi + \frac{x^{(2)}(\eta,t) - (x^{(1)}(\xi,t)}{h_n}\right) \\ &\underline{\mathbf{D}}(x^{(1)}(\xi,t) - h_n\psi)\underline{\mathbf{D}}^\top(x^{(1)}(\xi,t) - h_n\psi)(\nabla v^{(2)}(x^{(2)}(\eta,t)))^\top G_2^\top(s^*,\eta,t)dUd\eta d\xi \\ &+ \frac{1}{nh_n^3} \int_0^s \int_0^{s^*} \int_{\mathbb{R}^3} G_1(s,\xi,t)\nabla v^{(1)}(x^{(1)}(\xi,t))K(\psi)K\left(\psi + \frac{x^{(2)}(\eta,t) - x^{(1)}(\xi,t)}{h_n}\right) \\ &\Sigma_\Gamma(x^{(1)}(\xi,t) - h_n\psi)(\nabla v^{(2)}(x^{(2)}(\eta,t)))^\top G_2^\top(s^*,\eta,t)dUd\eta d\xi. \end{aligned}$$

Let $\eta = \xi + \tau h_n$. Then $d\eta = h_n d\tau$ and

$$\begin{aligned} &\frac{x^{(2)}(\eta,t) - x^{(1)}(\xi,t)}{h_n} \\ &= \frac{x^{(2)}(\xi + \tau h_n, t) - x^{(2)}(\xi,t) + x^{(2)}(\xi,t) - x^{(1)}(\xi,t)}{h_n} \\ &= \frac{\int_\xi^{\xi+\tau h_n} v^{(2)}(x^{(2)}(\zeta,t))d\zeta + \int_0^\xi v^{(2)}(x^{(2)}(\zeta,t))d\zeta - \int_0^\xi v^{(1)}(x^{(1)}(\zeta,t))d\zeta}{h_n} \to \infty \end{aligned}$$

as $h_n \to 0$. Thus, under any density kernel function, we have

$$\lim_{n\to\infty} \int_{\mathbb{R}^3} K(\psi)K\left(\psi + \frac{x^{(2)}(\eta,t) - x^{(1)}(\xi,t)}{h_n}\right)d\psi = 0.$$

Theorem 2 *Assumptions 1-3 hold. Consider the following testing problem for* $0 < a < b < T$

$$H_0 : \frac{\partial}{\partial t}\begin{bmatrix} x^{(1)}(s,t) \\ x^{(2)}(s,t) \end{bmatrix} = 0_6 \ \text{ against } \ H_1 : \frac{\partial}{\partial t}\begin{bmatrix} x^{(1)}(s,t) \\ x^{(2)}(s,t) \end{bmatrix} \neq 0_6, t \in [a,b].$$

For $s \in [0,S]$*, let*

$$\hat{W}_n(s) = \sqrt{nh_n^2}\Bigg\{ w^\top(b)\begin{bmatrix} \hat{x}_n^{(1)}(s,b) \\ \hat{x}_n^{(2)}(s,b) \end{bmatrix} - w^\top(a)\begin{bmatrix} \hat{x}_n^{(1)}(s,a) \\ \hat{x}_n^{(2)}(s,a) \end{bmatrix} - \int_a^b \left(\frac{d}{dt} w^\top(t)\right)\begin{bmatrix} \hat{x}_n^{(1)}(s,t) \\ \hat{x}_n^{(2)}(s,t) \end{bmatrix} dt \Bigg\},$$

where $w(t)$ *is a* 6×1 *vector-valued and time-dependent weight function. Under the null hypothesis* H_0*, the stochastic process* $\hat{W}_n(s), s \in [0,S]$ *converges weakly in the space of* $\mathbb{R}$*-valued continuous functions on* $[0,S]$ *to the Gaussian process* $\mathcal{GP}(s), s \in [0,S]$ *with mean function*

$$\mu(s) = w^\top(b)\begin{bmatrix} \mu_1(s,b) \\ \mu_2(s,b) \end{bmatrix} - w^\top(a)\begin{bmatrix} \mu_1(s,a) \\ \mu_2(s,a) \end{bmatrix} - \int_a^b \left(\frac{d}{dt} w^\top(t)\right)\begin{bmatrix} \mu_1(s,t) \\ \mu_2(s,t) \end{bmatrix} dt$$

and covariance function for $s, s^* \in [0,S]$

$$\begin{aligned} C(s,s^*) = {} & w^\top(b)\begin{bmatrix} C_{11}(s,s^*,b) & O_3 \\ O_3 & C_{22}(s,s^*,b) \end{bmatrix} w(b) \\ & + w^\top(a)\begin{bmatrix} C_{11}(s,s^*,a) & O_3 \\ O_3 & C_{22}(s,s^*,a) \end{bmatrix} w(a), \end{aligned}$$

where $\begin{bmatrix} \mu_1(s,t) \\ \mu_2(s,t) \end{bmatrix}$ *and* $\begin{bmatrix} C_{11}(s,s^*,t) & O_3 \\ O_3 & C_{22}(s,s^*,t) \end{bmatrix}$ *are defined as in Theorem 1.*

For finite points $s_1 < \cdots < s_m$ *in* $[0,S]$*, we define*

$$\hat{W}_0 = \begin{bmatrix} \hat{W}_n(s_1) \\ \hat{W}_n(s_2) \\ \cdots \\ \hat{W}_n(s_m) \end{bmatrix}, \quad \mu_0 = \begin{bmatrix} \mu(s_1) \\ \mu(s_2) \\ \vdots \\ \mu(s_m) \end{bmatrix}, \quad \text{and} \quad C_0 = \begin{bmatrix} C(s_1,s_1) & \ldots & C(s_1,s_m) \\ C(s_2,s_1) & \ldots & C(s_2,s_m) \\ \vdots & \ldots & \vdots \\ C(s_m,s_1) & \ldots & C(s_m,s_m) \end{bmatrix}.$$

Then we reject the null hypothesis H_0 *if*

$$[\hat{W}_0 - \mu_0]^\top C_0^+ [\hat{W}_0 - \mu_0] > \chi^2_{\alpha, df=k},$$

where A^+ *denotes the Moore-Penrose pseudoinverse of* A*,* $\chi^2_{\alpha,df=k}$ *is the critical value of the limiting chi-square distribution with* k *degrees of freedom at a significance level* α*, and* $k \leq m$ *is the rank of* C_0*.*

Sketch Proof of Theorem 2: Using the method of integration by parts, we note that

$$\hat{W}_n(s) = \sqrt{nh_n^2}\int_a^b w^\top(t)\frac{\partial}{\partial t}\begin{bmatrix} \hat{x}_n^{(1)}(s,t) \\ \hat{x}_n^{(2)}(s,t) \end{bmatrix} dt.$$

Under the null hypothesis, it can be rewritten as follows:

$$\begin{aligned} \hat{W}_n(s) &= \sqrt{nh_n^2}\int_a^b w^\top(t)\frac{\partial}{\partial t}\begin{bmatrix} \hat{x}_n^{(1)}(s,t) - x^{(1)}(s,t) \\ \hat{x}_n^{(2)}(s,t) - x^{(2)}(s,t) \end{bmatrix} dt \\ &= \sqrt{nh_n^2}\Bigg\{ w^\top(b)\begin{bmatrix} y^{(1)}(s,b) \\ y^{(2)}(s,b) \end{bmatrix} - w^\top(a)\begin{bmatrix} y^{(1)}(s,a) \\ y^{(2)}(s,a) \end{bmatrix} - \int_a^b \left(\frac{d}{dt} w^\top(t)\right)\begin{bmatrix} y^{(1)}(s,t) \\ y^{(2)}(s,t) \end{bmatrix} dt \Bigg\}, \end{aligned}$$

where $y^{(r)}(s,t) = \hat{x}_n^{(r)}(s,t) - x^{(r)}(s,t), r = 1,2$.

Let $y^{(r)}(s,t) = z^{(r)}(s,t) + \delta^{(r)}(s,t)$ as in the sketch proof of Theorem 1. Then we can decompose $\hat{W}_n(s) \overset{\text{under } H_0}{=} Z(s) + \Delta(s)$, where

$$Z(s) = \sqrt{nh_n^2}\Bigg\{ w^\top(b)\begin{bmatrix} z^{(1)}(s,b) \\ z^{(2)}(s,b) \end{bmatrix} - w^\top(a)\begin{bmatrix} z^{(1)}(s,a) \\ z^{(2)}(s,a) \end{bmatrix} - \int_a^b \left(\frac{d}{dt} w^\top(t)\right)\begin{bmatrix} z^{(1)}(s,t) \\ z^{(2)}(s,t) \end{bmatrix} dt \Bigg\}$$

and

$$\Delta(s) = \sqrt{nh_n^2}\Big\{ w^\top(b) \begin{bmatrix} \delta^{(1)}(s,b) \\ \delta^{(2)}(s,b) \end{bmatrix} - w^\top(a) \begin{bmatrix} \delta^{(1)}(s,a) \\ \delta^{(2)}(s,a) \end{bmatrix} - \int_a^b \left(\frac{d}{dt} w^\top(t) \right) \begin{bmatrix} \delta^{(1)}(s,t) \\ \delta^{(2)}(s,t) \end{bmatrix} dt \Big\}.$$

Then the rest of the proof is similar to the one of Theorem 2 in [10].

5. Discussion

In this article, we use the cosine of the angle between two tangent lines to the integral curves to investigate time-dependent anatomical changes in nerve fibers with two directions. Our future direction aligns with the application of real HARDI data based on our present theoretical work.

References

[1] M. S. Albert, S. T. DeKosky, D. Dickson, B. Dubois, H. H. Feldman, N. C. Fox, A. Gamst, D. M. Holtzman, W. J. Jagust, R. C. Petersen, P. J. Snyder, M. C. Carrillo, B. Thies, and C. H. Phelps. The diagnosis of mild cognitive impairment due to Alzheimer's disease: Recommendations from the national institute on aging-Alzheimer's association workgroups on diagnostic guidelines for Alzheimer's disease. *FOCUS*, 11(1):96–106, 2013.

[2] P. Basser, J. Mattiello, and D. LeBihan. Mr diffusion tensor spectroscopy and imaging. *Biophysical Journal*, 66(1):259–267, 1994.

[3] P. J. Basser, S. Pajevic, C. Pierpaoli, J. Duda, and A. Aldroubi. In vivo fiber tractography using dt-mri data. *Magnetic Resonance in Medicine*, 44(4):625–632, 2000.

[4] T. Behrens, M. Woolrich, M. Jenkinson, H. Johansen-Berg, R. Nunes, S. Clare, P. Matthews, J. Brady, and S. Smith. Characterization and propagation of uncertainty in diffusion-weighted mr imaging. *Magnetic Resonance in Medicine*, 50(5):1077–1088, 2003.

[5] B. B. Bendlin, M. L. Ries, M. Lazar, A. L. Alexander, R. J. Dempsey, H. A. Rowley, J. E. Sherman, and S. C. Johnson. Longitudinal changes in patients with traumatic brain injury assessed with diffusion-tensor and volumetric imaging. *NeuroImage*, 42(2):503–514, 2008.

[6] O. Carmichael and L. Sakhanenko. Estimation of integral curves from high angular resolution diffusion imaging (hardi) data. *Linear Algebra and its Applications*, 473:377–403, 2015.

[7] O. Carmichael and L. Sakhanenko. Integral curves from noisy diffusion mri data with closed-form uncertainty estimatesa. *Statistical Inference for Stochastic Processes*, 19:289–319, 2016.

[8] E. A. Coddington and N. Levinson. *Theory of ordinary differential equations*. McGraw-Hill, New York, 1955.

[9] M. Descoteaux, E. Angelino, S. Fitzgibbons, and R. Deriche. Apparent diffusion coefficients from high angular resolution diffusion imaging: Estimation and applications. *Magnetic resonance in medicine: an official journal of the international society for magnetic resonance in medicine*, 56(2):395–410, 2006.

[10] J. Goo, L. Sakhanenko, and D. C. Zhu. A chi-square type test for time-invariant fiber pathways of the brain. *Statistical Inference for Stochastic Processes*, 25(3):449–469, 2022.

[11] D. K. Jones. Determining and visualizing uncertainty in estimates of fiber orientation from diffusion tensor mri. *Magnetic Resonance in Medicine: An Official Journal of the International Society for Magnetic Resonance in Medicine*, 49(1):7–12, 2003.

[12] V. Koltchinskii, L. Sakhanenko, and S. Cai. Integral curves of noisy vector fields and statistical problems in diffusion tensor imaging: Nonparametric kernel estimation and hypotheses testing. *The Annals of Statistics*, 35(4):1576–1607, 2007.

[13] G. M. McKhann, D. S. Knopman, H. Chertkow, B. T. Hyman, C. R. Jack Jr., C. H. Kawas, W. E. Klunk, W. J. Koroshetz, J. J. Manly, R. Mayeux, R. C. Mohs, J. C. Morris, M. N. Rossor, P. Scheltens, M. C. Carrillo, B. Thies, S. Weintraub, and C. H. Phelps. The diagnosis of dementia due to Alzheimer's disease: Recommendations from the national institute on aging-Alzheimer's association workgroups on diagnostic guidelines for Alzheimer's disease. *Alzheimer's & dementia : the journal of the Alzheimer's Association*, 7(3):263–269, 2011.

[14] E. Özarslan and T. H. Mareci. Generalized diffusion tensor imaging and analytical relationships between diffusion tensor imaging and high angular resolution diffusion imaging. *Magnetic Resonance in Medicine*, 50(5):955–965, 2003.

[15] C. Poupon, C. A. Clark, V. Frouin, J. Regis, I. Bloch, D. Le Bihan, and J.-F. Mangin. Regularization of diffusion-based direction maps for the tracking of brain white matter fascicles. *Neuroimage*, 12(2):184–195, 2000.

[16] C. E. Sexton, K. B. Walhovd, A. B. Storsve, C. K. Tamnes, L. T. Westlye, H. Johansen-Berg, and A. M. Fjell. Accelerated changes in white matter microstructure during aging: a longitudinal diffusion tensor imaging study. *Journal of Neuroscience*, 34(46):15425–15436, 2014.

[17] D. S. Tuch, T. G. Reese, M. R. Wiegell, N. Makris, J. W. Belliveau, and V. J. Wedeen. High angular resolution diffusion imaging reveals intravoxel white matter fiber heterogeneity. *Magnetic Resonance in Medicine*, 48(4):577–582, 2002.

[18] L. Ying, Y. M. Zou, D. P. Klemer, and J.-J. Wang. Determination of fiber orientation in mri diffusion tensor imaging based on higher-order tensor decomposition. In *2007 29th Annual International Conference of the IEEE Engineering in Medicine and Biology Society*, pages 2065–2068, 2007.